GPS Solut (2015) 19:511–523
DOI 10.1007/s10291-014-0412-6

ORIGINAL ARTICLE

A wavelet-based hybrid approach to remove the flicker noise and the white noise from GPS coordinate time series

Hao Wu · Kui Li · Wenzhong Shi · Keith C. Clarke · Jianhua Zhang · Hua Li

Received: 17 April 2014 / Accepted: 24 September 2014 / Published online: 2 October 2014

Abstract Understanding the destructive interference of noise involved in GPS coordinate time series is crucial for improving the reliability of GPS applications. The majority of the noise consists of both flicker and white noise, both of which are well characterized by a stochastic process following a power-law noise model. To simplify the noise removal for GPS coordinate time series, the noise is usually regarded as pure white noise rather than a mixture of flicker noise and white noise. This work proposes a wavelet-based integrated solution that merges the strengths of Shannon entropy and wavelet thresholding to remove flicker and white noise at the same time. A GPS coordinate time series, spanning 128 days from the GPS monitoring station at the Jinduicheng Mine in Shanxi, China, was selected to test the proposed algorithm. The results demonstrate that both flicker noise and white noise are worthy of attention because they can lead to a seriously misunderstandings about error in a GPS coordinate time series. The utility of our proposed algorithm in removing flicker and white noise is shown to be more comprehensive than the use of wavelet thresholding alone. The findings further reveal that the advance elimination of flicker noise is beneficial for subsequently utilizing wavelet thresholding to delete the white noise in a GPS coordinate time series. This will greatly improve the reliability of GPS coordinate time series, allowing such data to be applied to a wide range of fields.

Keywords GPS · Coordinate time series · Denoise · Flicker noise · Shannon entropy · Wavelet transform

H. Wu · K. Li · J. Zhang · H. Li
School of Resources and Environmental Engineering, Wuhan University of Technology, Wuhan 430070, People's Republic of China

H. Wu · W. Shi (✉)
Department of Land Surveying and Geo-Informatics, The Hong Kong Polytechnic University, Hunghom, Kowloon, Hong Kong
e-mail: wenzhongshi1963@163.com; lswzshi@polyu.edu.hk

K. C. Clarke
Department of Geography, University of California, Santa Barbara, Santa Barbara, CA 93106-4060, USA

Introduction

Since it became fully operational in 1995, the global positing system (GPS) has been exploited to monitor geophysical phenomena, such as earthquakes, tectonic movements, and landslides. Its geodetic performance is intimately related to the satellite clock, terrain conditions, and atmospheric delay. Over the past 10 years, many algorithms have been proposed to mitigate performance error; however, they can still cause GPS positional determinations to be colored with noise that contains little or no geophysical information (Senior et al. 2008; Shi et al. 2012; Tregoning and Watson 2011). Thus, it is crucial to remove noise to improve the reliability of GPS coordinate time series data.

While GPS uses a variety of methods and measurements to determine a geographic position's location and elevation, we consider the final positional estimate {x, y, z, and t} as the measurement in question. At a fixed location, {x, y, and z} should be constant for any sampling frame for t, but in reality, the entire GPS error budget (Leick 2004) means that {x, y, and z} can only converge on a "true" location. This is especially important when subtle small changes in {x, y, and z} are anticipated, or when they need to be invariant during their use as positional control. A series of {x, y, and z} processed measurements in grid coordinate units such as latitude and longitude and height

above a datum, sampled across time t at a uniform interval, is what we term a GPS coordinate time series. As with many other geophysical phenomena, the noise contained in GPS coordinate time series can be described by a power-law function (Mandelbrot 1983). Agnew (1992) has demonstrated that the noise involves not only independent and identically distributed white noise but also the flicker noise that is characterized by non-stationary variation and long-term interaction. The source of this flicker error can be multi-path errors, upper atmosphere conditions, changes in the surrounding topography, ephemeris, and clock updates, GPS epoch change, and other sources. Williams et al. (2004) also indicate that the noise in GPS coordinate time series can be best described by a combination of flicker and white noise. Actually, the denoising for GPS coordinate time series dates back to the early work on white noise. Flicker noise is generally not considered during noise removal for GPS coordinate time series (Huang and Fu 2007). Past studies regarded the hybrid noise contained in GPS coordinate time series as pure white noise (Santamaria-Gomez et al. 2011). Nevertheless, the recent development of effective noise removal algorithms revealed that a serious bias could radically affect subsequent analysis and results if we disregard flicker noise. Several studies have recognized flicker noise besides white noise in GPS coordinate time series (Nikolaidis et al. 2001; Teferle et al. 2008; Amiri-Simkooei and Tiberius 2007; Amiri-Simkooei et al. 2007; Amiri-Simkooei 2009). All of them indicate that the reliability of GPS coordinate time series is significantly disturbed by both flicker and white noise. Thus, it is important to remove flicker noise as well as the white noise in GPS coordinate time series if high precision and accuracy are important for an application.

Wavelet theory has been used for its potential to remove flicker and white noise in GPS coordinate time series. In terms of white noise, Montillet et al. (2013) have proved that the white noise in GPS coordinate time series is independent and identically distributed. It is generally associated with hardware noise or measurement errors inherent in the GPS system, for example, in the precision and repeatability of the atomic clocks, or the time length of a discrete pseudorange encoding. Those errors can bring centimeter-level biases to the subsequent analysis and results even in high-end survey/geodesy grade GPS equipment. However, many civil engineering applications related to GPS coordinate time series, such as slope deformation monitoring and tectonic plate movement, require millimeter-level accuracy (Wu et al. 2011). The existence of white noise seriously affects the accuracy and reliability of GPS coordinate time series.

Donoho (1995) found wavelet thresholding to be a significantly effective technique for removing white noise in GPS coordinate time series. Based on the theory of Donoho, many studies have proposed new methods to improve the quality of the GPS positional signals. For instance, Gao (1997) presents the thresholding level to make the reconstructed log spectrum as nearly noise-free as possible. Souza and Monico (2004) used wavelet shrinkage to reduce the high frequency multi-path error in GPS relative positioning. Although both studies made a contribution to GPS noise removal, they failed to take into account improvement due to the smoothness of the long-term GPS signals. In order to make up this defect, Han et al. (2007) presented a new thresholding algorithm to smooth noise for a nonlinear time series based on the wavelet soft threshold. Approaches to eliminate flicker noise from GPS coordinate time series have also been the focus of research. Flicker noise has distinct statistical properties when compared to white noise. He and Wang (2003) have indicated that flicker noise is characterized by non-stationary variation and long-term interaction. It is no longer applicable for us to analyze flicker noise with the traditional methods for white noise. Yet, the elimination of flicker noise has not yet been attained. Flicker noise embedded in white background noise can be removed based on information theory using Shannon's entropy as discussed by He and Wang (2003), but white noise was not considered during their analysis. In addition, Wornell and Oppenheim (1992) utilized the maximum likelihood in the wavelet domain to estimate the flicker noise from GPS station coordinate time series. Chen and Lin (1994) applied orthonormal wavelets, together with a multi-scale Wiener filter, to remove the flicker noise in GPS coordinate time series. The aforementioned studies show that wavelet theory has the potential to remove both flicker and white noise in GPS coordinate time series. Despite these significant contributions of wavelet theory to eliminate flicker and white noise from GPS coordinate time series, no substantial research has yet attempted to simultaneously remove them using a wavelet-based hybrid approach. However, the ability of any single wavelet-based approach to completely remove both types of noise in GPS coordinate time series is too limited.

The main objective of this paper is to investigate how best to use a wavelet-based hybrid approach to remove both the flicker and white noise contained in GPS coordinate time series. A general framework for eliminating the noise in GPS coordinate time series is given, which includes the following: (1) the elimination of flicker noise embedded in white background noise based on Shannon entropy, and (2) the removal of white noise using wavelet thresholding. In particular, a wavelet-based integrated solution is presented that merges the strengths of Shannon entropy and wavelet thresholding to eliminate these two kinds of noises in time series. By eliminating both types of noise, we can greatly improve the reliability and value of GPS coordinate time series.

Methods

The majority of current noise removal methods pay more attention to the elimination of white noise than flicker noise. In this section, we propose a wavelet-based hybrid approach to efficiently eliminate both flicker noise and white noise.

The general framework for denoising GPS coordinate time series

Figure 1 shows that the general framework for removing both flicker and white noise in GPS coordinate time series is composed of a two-step processing chain, including (1) deleting the flicker noise embedded in white background noise based on Shannon entropy; and then (2) applying wavelet thresholding to eliminate the white noise contained in the positional signal.

The flicker noise embedded in white background noise was extracted from GPS coordinate time series by Shannon entropy. The initial signal was first transformed from the spatial domain to the frequency domain and the signal-to-noise ratio (SNR) estimated. This SNR was used to generate the artificial white noise W_N that can be used to represent the real white noise (Ma et al. 2002). We utilized the wavelet transform to obtain the wavelet coefficients of the artificial white noise ω_i^j and calculated the modulus maxima series $\overline{\omega_k^j}$. Then, the Shannon entropy of the wavelet coefficients of the artificial white noise $E_n[\overline{\omega_k^j}]$ was computed (He and Wang 2003). Similarly, the wavelet coefficients r_i^j, the modulus

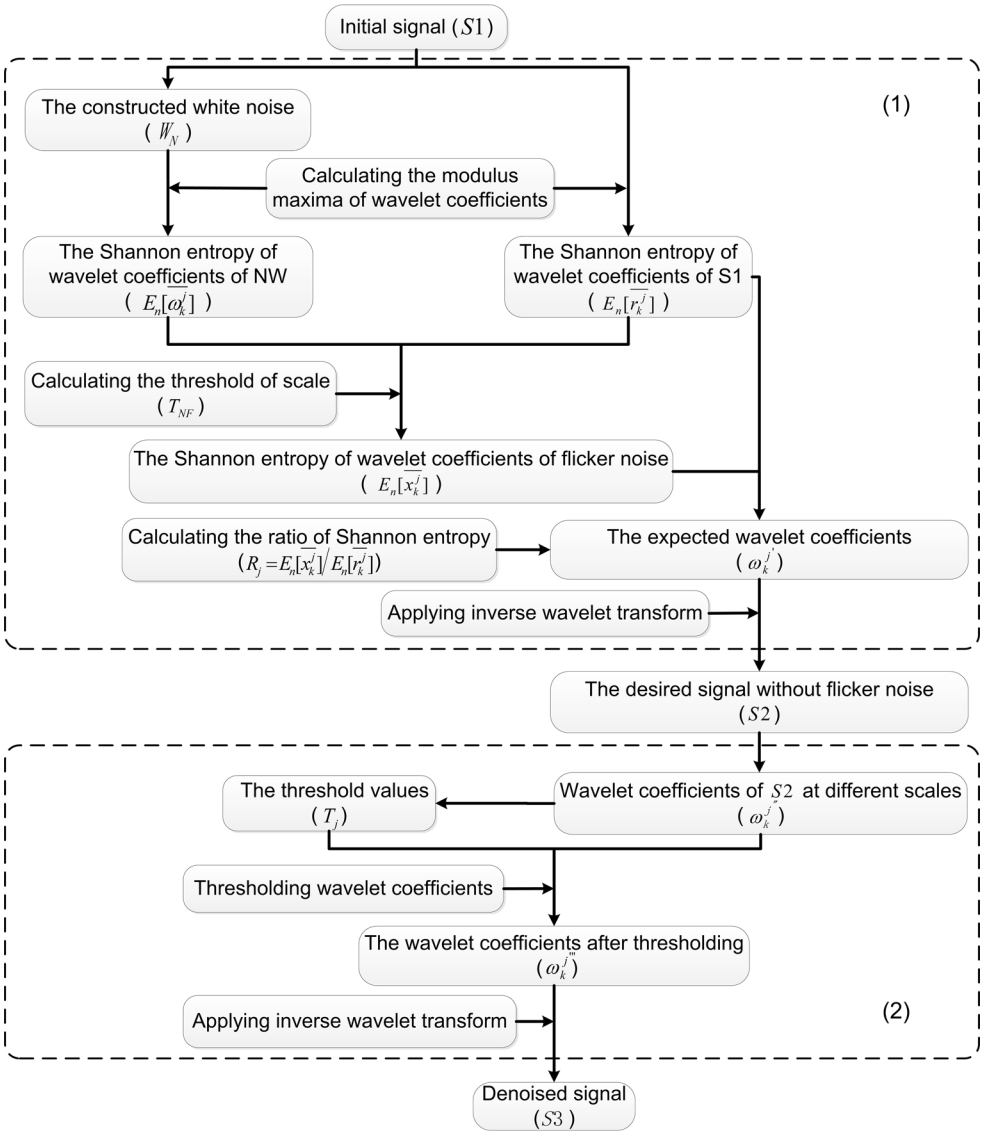

Fig. 1 General framework for denoise GPS station coordinate time series

maxima series $\overline{r_k^j}$ and the Shannon entropy of the wavelet coefficients of the initial signal $E_n[\overline{r_k^j}]$ were also computed. Following the calculation of the threshold of scale T_{NF}, we computed the Shannon entropy of the wavelet coefficients of the flicker noise $E_n[\overline{x_k^j}]$ by the relationship between $E_n[\overline{r_k^j}]$ and $E_n[\overline{\omega_k^j}]$. The expected wavelet coefficients $\omega_i^{j'}$ were computed with the aid of the Shannon entropy ratio $\overline{R_j}$ of the flicker noise to the initial signal at different scales. Finally, we reconstructed the signal $S2$ without the flicker noise from the expected wavelet coefficients $\omega_i^{j'}$.

To further eliminate the white noise existing in signal $S2$, we utilized wavelet thresholding. This approach is required to decompose the signal $S2$ into the wavelet coefficients $\omega_i^{j''}$ and to calculate the threshold values T_j, which depend on the variance of $\omega_i^{j''}$ and the sample size. We then calculated the wavelet coefficients $\omega_i^{j'''}$ by deleting the wavelet coefficients having a modulus less than T_j. Thus, the denoised signal $S3$ was reconstructed from the coefficients $\omega_i^{j'''}$ using the inverse wavelet transform.

The Shannon entropy-based flicker noise elimination

Because the flicker noise has a distinct statistical significance that is different from that of other signals, traditional methods such as wavelet thresholding, wavelet shrinkage denoising and Kalman filters are not suitable to denoise the flicker noise. It has been demonstrated that information entropy can quantify the information expected value of the flicker noise contained in a signal (Fu 2001). We can use this value to extract the flicker noise from GPS coordinate time series by utilizing the relationship between $E_n[\overline{r_k^j}]$ and $E_n[\overline{\omega_k^j}]$. Actually, the Shannon entropy of the wavelet coefficients of the real white noise found in GPS coordinate time series is only related to the variance of the real white noise at the same scale. The variance δ_w^2 of the real white noise was derived from the SNR of $S1$. Thus, we calculated the Shannon entropy of the wavelet coefficients using the artificial white noise W_N rather than the real white noise (Ma et al. 2002). The wavelet coefficients of white noise ω_i^j were computed by the wavelet transform as follows:

$$\omega_i^j = \int_{-\infty}^{\infty} W_N(t)\psi_i^j(t)\,\mathrm{d}t \tag{1}$$

With the mother wavelet function

$$\psi_i^j(t) = 2^{-j/2}\psi(2^{-j}t - i) \tag{2}$$

where j is the scale and i is the position of the wavelets. The size of W_N is $N = 2^J$, and the corresponding index is $\{(j,i), \quad j = 0,\ldots,J-1, \quad i = 0,\ldots,2^j - 1\}$; $\psi(t)$ is the mother wavelet equation. Then, we calculated its modulus maxima $\overline{\omega_k^j}$ to estimate $E_n[\overline{\omega_k^j}]$. It was simplified to the following equation:

$$E_n[\overline{\omega_k^j}] = -\sum_k (\overline{\omega_k^j})^2 \log_2[(\overline{\omega_k^j})^2] \tag{3}$$

where k denotes the number of the modulus maxima. So $\overline{r_k^j}$ and $E_n[\overline{r_k^j}]$ at different scales were calculated in the same way. The Shannon entropy values of the wavelet coefficients of the flicker noise $E_n[\overline{x_k^j}]$ at different scales were then determined by the relation:

$$E_n[\overline{x_k^j}] = \begin{cases} E_n[\overline{r_k^j}] - E_n[\overline{\omega_k^j}] & (j < T_{\mathrm{NF}}) \\ E_n[\overline{r_k^j}] & (j \geq T_{\mathrm{NF}}) \end{cases} \tag{4}$$

where $\overline{x_k^j}$ is the modulus maxima series of the wavelet coefficients for the flicker noise at scale j. T_{NF} is the threshold of scale, which is determined by the ratio $R_j = E_n[\overline{r_k^j}] \Big/ E_n[\overline{\omega_k^j}]$. We used the ratio $\overline{R_j} = E_n[\overline{x_k^j}] \Big/ E_n[\overline{r_k^j}]$ to calculate the expected wavelet coefficients $\omega_i^{j'}$ that is defined by the following:

$$\omega_i^{j'} = (1 - \overline{R_j})\, r_i^j \tag{5}$$

Finally, we utilized the inverse wavelet transform to reconstruct the signal $S2$ of GPS station coordinate time series, in which the flicker noise has been removed. The corresponding equation is given by the following:

$$S2 = \sum_j \sum_i \omega_i^{j'} \psi_i^j(t) \tag{6}$$

where $S2$ is the signal in which the flicker noise has been removed from the initial signal $S1$, and $\omega_i^{j'}$ are the expected wavelet coefficients of signal $S2$.

Wavelet thresholding-based white noise elimination

Wavelet thresholding was originally proposed by Donoho (1995) to remove white noise from a given signal. The authors deleted the wavelet coefficients of the white noise when its modulus was less than a given threshold. Then, they made use of the remaining coefficients to reconstruct the denoised signal by taking the inverse wavelet transform. By Eq. (1), we decomposed the signal $S2$ into the wavelet coefficients $\omega_i^{j''}$. The wavelet coefficients $\omega_i^{j'''}$ were determined through a soft thresholding rule:

$$\omega_i^{j'''} = \eta_S\left(\omega_i^{j''}, T_j\right) = \begin{cases} \omega_i^{j''} - T_j & \left(\omega_i^{j''} \geq T_j\right) \\ 0 & \left(\left|\omega_i^{j''}\right| < T_j\right) \\ \omega_i^{j''} + T_j & \left(\omega_i^{j''} - T_j\right) \end{cases} \tag{7}$$

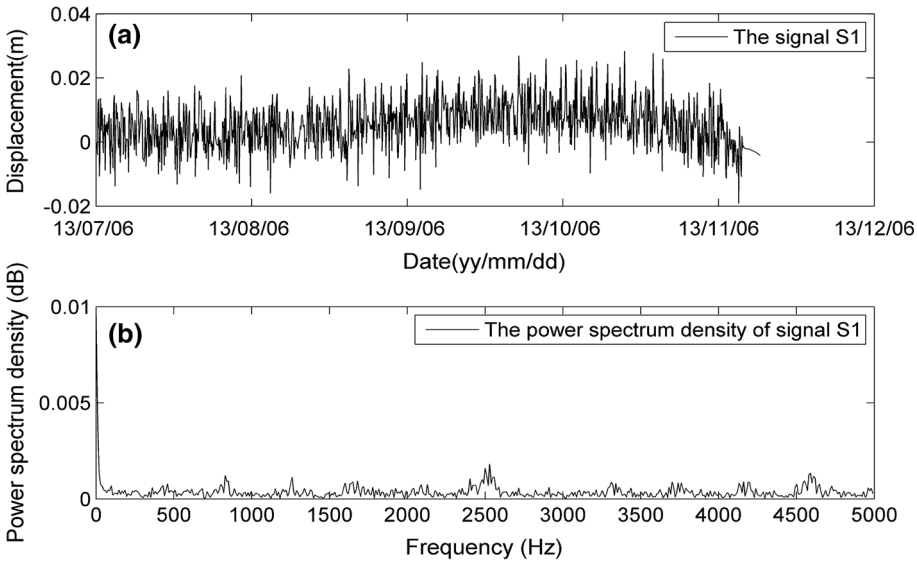

Fig. 2 The initial signal $S1$ at the time domain and frequency domain: **a** the displacement time series of S1 from 13/07/06 to 13/11/11, and **b** the result of a fast Fourier transform

In Eq. (7), T_j denotes the given threshold and is estimated by the following equation (Han et al. 2007):

$$T_j = \sigma_j \sqrt{2 \ln N} \tag{8}$$

where σ_j is the variance of the detail coefficients at scale j, and N is the total number of points. Finally, the denoised signal $S3$ of GPS coordinate time series, which excludes both the flicker noise and the white noise, was calculated by taking the inverse wavelet transform.

Case study of the proposed algorithm in a molybdenum mine

Jinduicheng Mine is the largest molybdenum production source in China. It is located in Weinan city, Shanxi Province, northwest China, at 34°25′N 109°57′E. The mining area is approximately 4.5 km^2. There is a large number of slopes in the mining area, with dip angles from 35° to 45° which seriously affect the safety of the mining area, and thus, it is necessary to continuously monitor slope stability (Wu et al. 2013; Zhao et al. 2013). For this reason, a GPS-based continuous monitoring network was established in 2012, which performs the data collection for safety assessment (Wang et al. 2011). The system provides 3D coordinates {x, y, and z} for each monitoring station once every 3 h. Thus, the displacement time series from each monitoring station is available to monitor the slope stability during a continuous monitoring period. Unfortunately, it cannot directly quantify the trend of displacement change for a given monitoring station within the given cycle, due to the existence of errors. As shown in Fig. 2a, the z-direction displacement time series collected from July 6, 2013 (13/07/06) to November 11, 2013 (13/11/11) contains significant errors, making the deformation trend difficult to conveniently and accurately understand. As for the errors in GPS coordinate time series, many publications since 1997 (Langbein and Johnson 1997; Mao et al. 1999; Williams et al. 2004) have proven that the errors in GPS coordinate time series are mainly composed of both white noise and flicker noise. It provides us with sufficient experiment guidance to assert that a combination of flicker and white noise is the best model for the noise in GPS coordinate time series. Therefore, we assume the error in our data as the combination of flicker and white noise.

A monitoring station (DB05), which has the most typical displacement among all of the monitoring stations, was selected as a case study of the proposed algorithm. Figure 2a shows that the displacement time series has 1,024 samples as the initial signal $S1$. Although accurate observation coordinates for a given sample point are available once every 3 h, we cannot estimate the displacement trend during the monitoring phase. Thus, we made use of the proposed algorithm to remove the types of noise contained in the coordinate time series. To further validate the existence of the noise, the signal was transformed from the time domain to the frequency domain using the fast Fourier transform (FFT). It has been known that the signal always lies in the low frequency range, while the noise lies in the high frequency range (Zhang et al. 2006). Figure 2b shows that there is a notable power spectral density within the high frequency range ($\geq$50 Hz) compared with that of the low frequency range ($<$50 Hz). This means that the quality of the initial signal $S1$ is seriously affected by the noise.

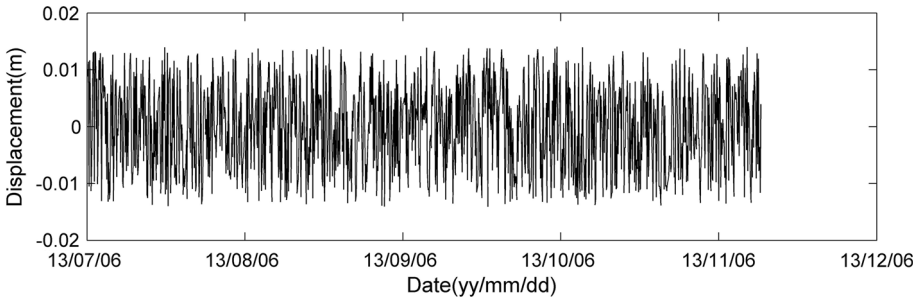

Fig. 3 Artificial white noise generated from the variance of the real white noise

Results

In this section, we will give the denoising results of the initial signal $S1$ that was collected by the monitoring station (DB05) spanning 128 days from 13/07/06 to 13/11/11. It is described as three parts, including (1) the simulation result of artificial white noise, (2) elimination of flicker noise, and (3) the denoised GPS coordinate time series.

The simulation result of artificial white noise

To calculate the Shannon entropy of the wavelet coefficients of the real white noise $E_n[\overline{\omega_k^j}]$, we need to simulate the artificial white noise W_N in advance and then substitute it for the real white noise. Because the $E_n[\overline{\omega_k^j}]$ is only related to the variance of the real white noise at a certain scale, it is reasonable to generate the approximate artificial white noise from the variance of the real white noise. The artificial white noise can be built by using the rand function of MATLAB. Figure 3 shows the simulation result of the artificial white noise that ranges in amplitude from -0.015 to 0.015 m. It belongs to a random distribution with a mean value of 0 and a variance $\delta_w^2 = 6.5974 \times 10^{-5}$. This suggests that it is in a good accord with the characteristics of the actual white noise. In addition, Ma et al. (2002) have indicated that the Shannon entropy of the wavelet coefficients of the real white noise found in GPS coordinate time series is only related to the variance δ_w^2 of the real white noise at the same scale. Thus, the utilization of different artificial white noises with the same variance δ_w^2 for replacing the real white noise cannot affect the resulting SNR. Although we have theoretically shown that the artificial white noise can be used to calculate $E_n[\overline{\omega_k^j}]$ instead of the real white noise, we cannot fully rule out the possibility that it may be affected by other factors, resulting in the failure of this substitution. In this regard, the feasibility of using artificial white noise to replace the real white noise for subsequent computations is demonstrated by the accuracy of the following result.

Elimination of flicker noise

The Shannon entropy is a good measure of the information content (Shannon 1948). In this study, it was used to determine the proportion of the wavelet coefficients of the flicker noise to the initial signal at different wavelet decomposition scales. This requires calculating the Shannon entropy of the wavelet coefficients for different signals at each wavelet decomposition scale. Table 1 lists the original signal entropy $\left(E_n[\overline{r_k^j}]\right)$ and the white noise entropy $\left(E_n[\overline{\omega_k^j}]\right)$ at different wavelet decomposition scales (R_j).

As shown in Table 1, $E_n[\overline{r_k^j}]$ is large (approximately 0.9) at low scales and levels off around the value of 0.09 at high scales. The value of $E_n[\overline{\omega_k^j}]$ varies from 0.7856 to 0.0077, as the wavelet decomposition scale increases from the minimum scale to 8. Furthermore, $E_n[\overline{\omega_k^j}]$ becomes lower so that it is usually ignored when the scale reaches the threshold of scale T_{NF} defined in Eq. (4). This threshold is determined by the change of $R_j = E_n[\overline{r_k^j}] \big/ E_n[\overline{\omega_k^j}]$ at different scales. Figure 4 shows how the numerical values of the ratio R_j directly respond to the increasing wavelet decomposition scale. We see that the ratio R_j gradually increases first from 1.6840 to 4.8848 as the wavelet decomposition size increases to the scale of 6 and then sharply grows up around the value of 10.9959 at the scale of 7. Finally, the ratio R_j returns to steadily increase again at the wavelet decomposition size of 7 and 8. This indicates that $E_n[\overline{\omega_k^j}]$ can be neglected compared with $E_n[\overline{r_k^j}]$ when the scale is beyond 6. This means that the threshold of scale T_{NF} is equal to 6.

Given the existence of relationship between $E_n[\overline{r_k^j}]$ and $E_n[\overline{\omega_k^j}]$ as demonstrated above, $E_n[\overline{x_k^j}]$ was calculated by Eq. (4). The related results at different wavelet decomposition scales are given in Table 2. In analyses with the two datasets, we can find that $E_n[\overline{x_k^j}]$ varies between 0.0995 and 0.5387 and $\overline{R_j}$ falls in between 0.1441 and 1. In addition, $\overline{R_j}$

Table 1 $E_n[\overline{\omega_k^j}]$, $E_n[\overline{r_k^j}]$, and Rj at different scales

Scale	1	2	3	4	5	6	7	8
$E_n[\overline{r_k^j}]$	0.9179	1.1028	0.6512	0.5214	0.2307	0.2926	0.2661	0.0995
$E_n[\overline{\omega_k^j}]$	0.7856	0.5641	0.3592	0.1926	0.0985	0.0599	0.0242	0.0077
R_j	1.1684	1.9550	1.8129	2.7212	2.3421	4.8848	10.9959	12.9880

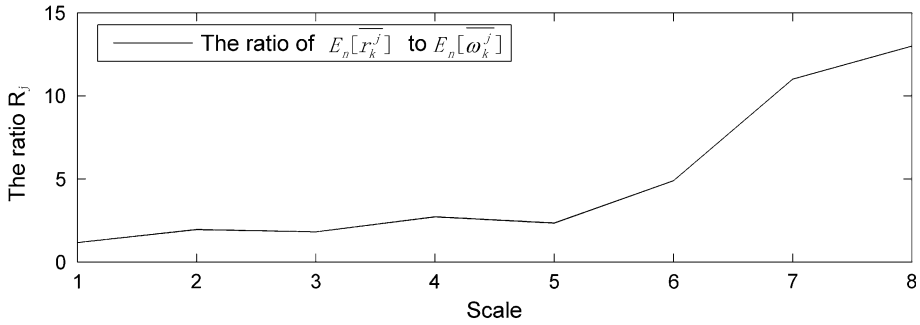

Fig. 4 Change of the ratio of the Shannon entropy of wavelet coefficients of the initial signal $E_n[\overline{r_k^j}]$ to white noise $E_n[\overline{\omega_k^j}]$ at different wavelet decomposition scales

Table 2 $E_n[\overline{x_k^j}]$ and $\overline{R_j}$ at different scales

Scale	1	2	3	4	5	6	7	8
$E_n[\overline{x_k^j}]$	0.1323	0.5387	0.2920	0.3315	0.1322	0.2684	0.2611	0.0995
$\overline{R_j}$	0.1441	0.4885	0.4484	0.6325	0.5732	0.7953	1	1

exhibits a nearly linear increase as the wavelet decomposition scale rises up to the scale of 8. This suggests that the proportion of the wavelet coefficients of the flicker noise increases with increasing wavelet decomposition scale. Thus, the expected wavelet coefficients $\omega_i^{j'}$ can be determined according to Eq. (5). The reconstructed signal $S2$, which is the initial signal $S1$ with the flicker noise removed, is shown in Fig. 5a. There was no obvious improvement to the smoothness of the signal $S2$ (Fig. 5a) compared with that of the initial signal $S1$ (Fig. 2a). Nevertheless, Fig. 5b shows the FFT result for the signal $S2$, which is distinctly different when compared to $S1$ (Fig. 2b). There is a significant decrease in the power spectral density within the high frequency range ($\geq$50 Hz) of the signal $S2$ (Fig. 5b) compared with that of the initial signal $S1$ (Fig. 2b). Moreover, the power spectral densities within the low frequency range (<50 Hz) of both signals remain unchanged. This implies that the quality of the signal $S2$ has greatly improved when the flicker noise is eliminated from the initial signal $S1$.

The denoised GPS coordinate time series

The best model of the noise characteristics in the time series of a given GPS station can be described as the combination of the white noise and the flicker noise. The flicker noise contained in the initial signal has been eliminated in the section of the elimination of flicker noise. Despite some improvements of signal smoothness, the result shown in Fig. 5a does not achieve a great success. The reason for this failure is because the signal $S2$ still contains white noise. This leads to the fact that we cannot directly examine the height or z displacement trend of the monitoring station from 13/07/06 to 13/11/11. So it is necessary to remove the white noise from the signal $S2$. Unlike the flicker noise, the white noise in the signal $S2$ can be removed by directly applying wavelet thresholding. Figure 5c shows the displacement time series of signal $S3$, which is calculated utilizing wavelet thresholding and contains the signal $S2$ with the white noise removed. Now, the signal $S3$ contains neither the flicker noise nor the white noise. As shown in Fig. 5c, it is evident that the smoothness of signal $S3$ is greater than that of signal $S2$ (Fig. 2a). Thus, the displacement trend of the monitoring station within the given cycle can be more accurately quantified rather than if the initial signal $S1$ or the signal $S2$ is used. Comparing Figs. 2a and 5c, we show that the proposed algorithm significantly enhances the smoothness of the initial signal $S1$. In addition, although the power spectral density within the low frequency range (<50 Hz) remains unchanged, there is a sharp contrast to signals $S2$ and $S3$ at about the power spectral density within the high frequency

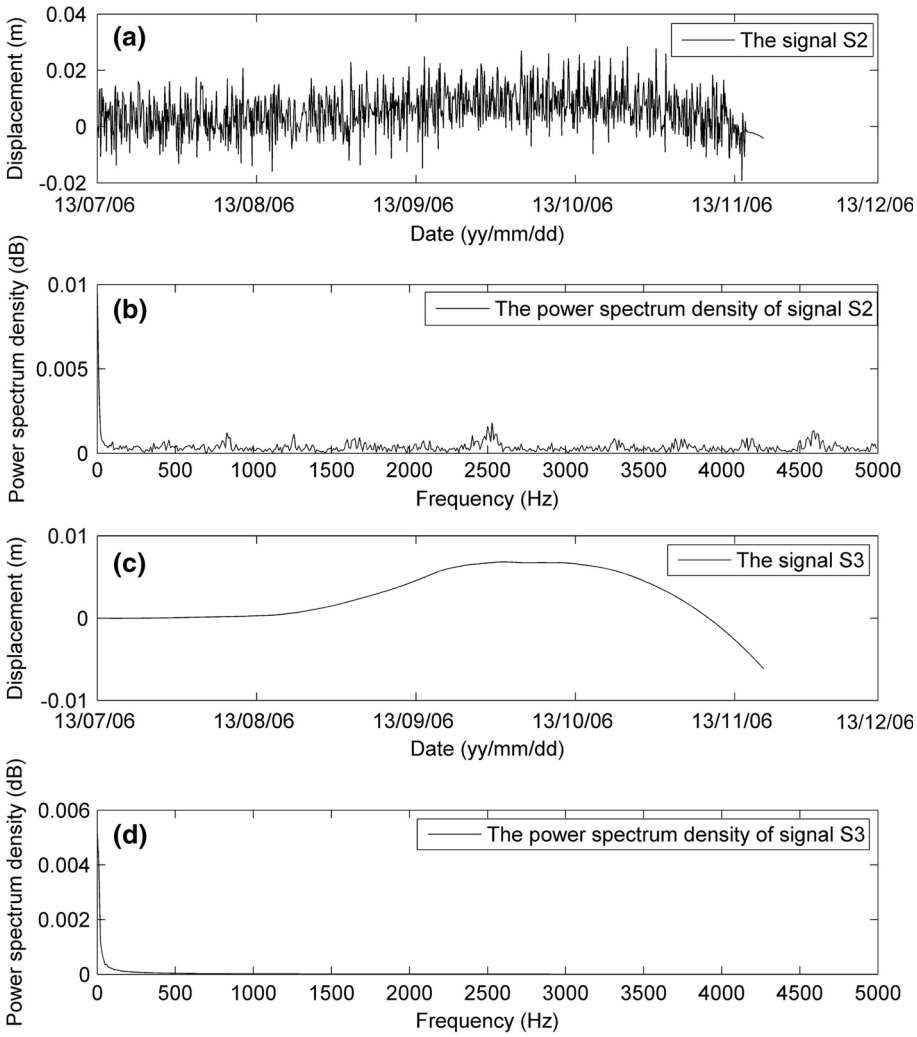

Fig. 5 Results of *S*2 (excluding the flicker noise from *S*1) and *S*3 (excluding both flicker and white noise from *S*2) using the proposed algorithm: **a** the displacement time series of *S*2 from 13/07/06 to 13/11/11, **b** the result of a FFT derived from signal *S*2, **c** the displacement time series of *S*3 from 13/07/06 to 13/11/11, and **d** the result of fast Fourier transform derived from signal *S*3

range (≥50 Hz). This suggests that the quality of the signal *S*3 has been greatly improved when we use the proposed algorithm to remove both flicker and white noise. The results shown in Fig. 5 are consistent with this view that the noise in GPS coordinate time series can be well described by a combination of flicker and white noise. However, with the development of the multi-constellation receiver in many fields, the noise from GNSS-based coordinate time series becomes more and more complicated than that of the sole-GPS navigation. This perhaps greatly affects the reliability of coordinate time series.

Discussion

In this section, we will discuss the denoising results of the GPS coordinate time series in details to illustrate the superiority of the wavelet-based hybrid method. It will be compared with the wavelet thresholding in smoothness and the signal-to-noise ratio. In addition, we will test the flicker noise eliminated from signal *S*2.

The complexity of noise in GPS coordinate time series

There are some traditional denoising methods (e.g., wavelet thresholding, wavelet shrinkage denoising, and Kalman filters) that usually regard the noise involved in GPS coordinate time series as pure white noise rather than as a combination of flicker and white noise (Azzalini et al. 2005; Donoho and Johnstone 1994; Geng and Wang 2008). To comprehensively demonstrate the necessity of removing the flicker noise from GPS coordinate time series, we compared wavelet thresholding with our proposed algorithm. Because wavelet thresholding was applied to eliminate the white noise from the signal *S*2 in the proposed algorithm, we chose this technique to denoise the initial signal in this section to make the result more comparable. Figure 6a shows the displacement time series of signal *S*4, where the

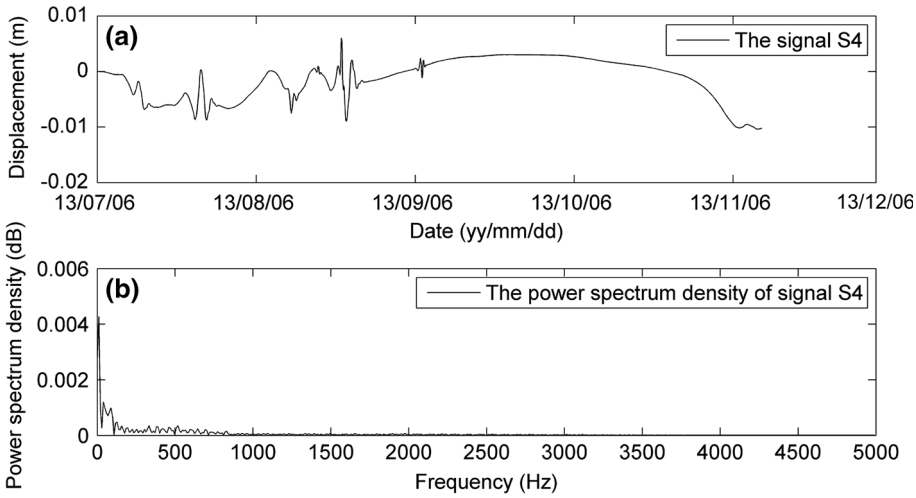

Fig. 6 Result of *S*4 (only excluding the white noise from *S*1) using wavelet thresholding: **a** the displacement time series of *S*4 from 13/07/06 to 13/11/11, and **b** the result of fast Fourier transform

white noise has been eliminated from the initial signal *S*1 using wavelet thresholding. As shown in Figs. 5c and 6a, we can find that there is a significant difference on the deformation trend between our proposed method and the traditional method. There is no doubt that the smoothness of signal *S*4 is inferior when compared to signal *S*3. It is clear that we cannot directly make use of signal *S*4 to analyze the real historical displacement or to predict the probable future displacement trend for a given monitoring station. The FFT of signal *S*4 is given in Fig. 6b. We find that the degree of the power spectral density within the high frequency range ($\geq$50 Hz) for the signal *S*4 drops less appreciably than that for the signal *S*3, under the condition that each of their power spectral densities within the low frequency range (<50 Hz) remains unaffected. This suggests that signal *S*1 involves a combination of the white noise and other uncertain noise, but not the white noise alone. On the basis of the analysis above, we conclude that a more sophisticated noise model is necessary if we seek to fully denoise a GPS coordinate time series.

Validation of the flicker noise

The flicker noise that was eliminated from the initial signal *S*1 by the proposed algorithm is shown in Fig. 7a. As for the flicker noise, it has been reported that the relationship between the logarithm of power spectral density ln *S* and the logarithm of frequency ln *F* follows the characteristic of an inverse function (Williams 2008; Williams et al. 2004). According to the above-mentioned literature (Montillet et al. 2013), the noise can be regarded as flicker noise when its regression line slope between ln *S* and ln *F* is equal to -1. A statistically significant relationship between ln *S* and ln *F* was established using linear regression analyses, as shown in Fig. 7b, allowing us to examine whether the noise removed from the initial signal *S*1 can be attributed to the flicker noise. Figure 7b shows that the correlation coefficient R^2 derived from the least-squares estimation for the flicker noise is 0.9408. This suggests that there is a significant linear relationship between ln *S* and ln *F*. For this reason, we can use the result of the linear regression fitting to judge whether the noise is flicker noise. Figure 7b shows that the slope of the linear regression equation is equal to -1.1362 with an approximation to -1. It means that the noise shown in Fig. 7a that has been removed from the initial signal *S*1 pertains to flicker noise.

Quantitative comparison of the signal quality

Although both the smoothness and the power spectral density within the high frequency range ($\geq$50 Hz) for different signals has already been touched upon earlier in the discussion results, it is not a readily intuitive means of expressing the change in the different signals' quality. To further advance our understanding of the quality change of different signals in the denoising process, we utilized the measure of the SNR to highlight their individual differences. Figure 8 shows the estimation of the SNR for all four signals of the 1,024-point time series. Of all these four signals, the signal *S*3 achieves the best performance in terms of the SNR. It suggests that the proposed algorithm performs better than white noise-only methods with respect to improving the SNR of the signal. Additionally, the SNR of signal *S*2 is equal to 0.8866 dB, which is nearly 3 times that of initial signal *S*1, while the SNR of signal *S*3 is approximately 6 times that of signal *S*2. This is mainly due to the reason that the characteristics of white noise become more clear after we remove the flicker noise from the signal S1 using our proposed method.

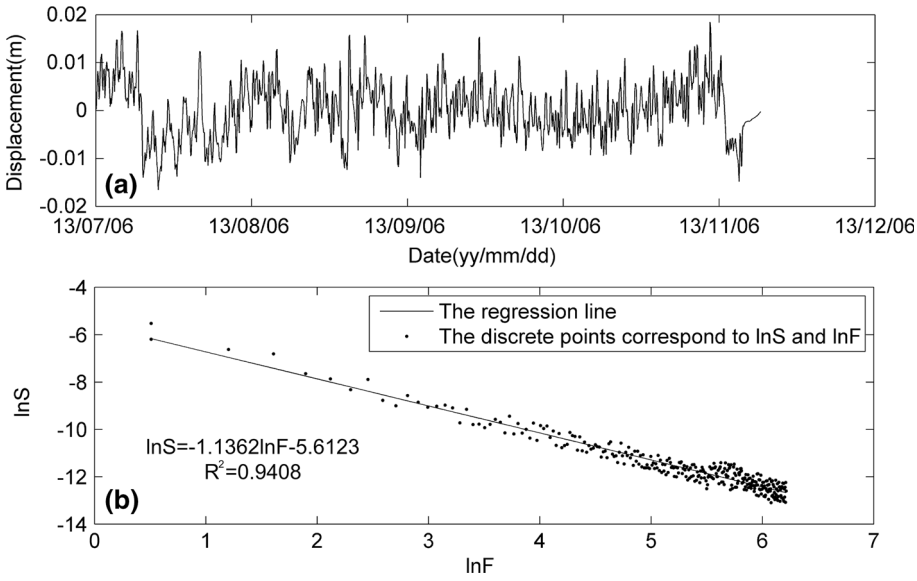

Fig. 7 Result of the flicker noise that is removed from signal *S*1: **a** the displacement time series of the flicker noise from 13/07/06 to 13/11/11, **b** the regression line and discrete points corresponding to ln *S* and ln *F*

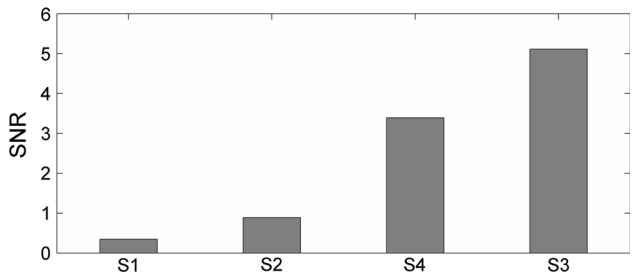

Fig. 8 Comparison result of different signals in signal-to-noise ratio (SNR)

Removing flicker noise greatly improves the efficiency of the traditional wavelet threshold method for the elimination of white noise. In addition, different noises that lie in original information have a mutual influence. That is to say, a certain noise not only affects the quality of original information, but also has a potential impact on other noise that may enlarge the effect on the signal with a nonlinear propagation. This indicates that the elimination of flicker noise in advance is beneficial for deleting the white noise in GPS coordinate time series. And it could easily result in the spurious argument that the elimination of the flicker noise is not needed with respect to that of the white noise. However, Fig. 8 shows that the SNR of signal *S*4 is equal to 3.3894 dB if we just remove the white noise without considering the existence of the flicker noise. It suggests that the colored noise does not obviously show the characteristics of white noise and flicker noise. This seriously affects the efficiency of the traditional methods to eliminate white noise. From the result discussed above, it is clear that neglecting to remove the flicker noise significantly affects the denoised result for the white noise. Hence, the advance elimination of the flicker noise from GPS coordinate time series, in general, can greatly enhance the denoising procedure for the white noise.

Conclusions

The noise in GPS coordinate time series can be described by a combination of flicker and white noise. Traditionally, however, we pay more attention to the white noise and ignore the existence of flicker noise during the denoising of GPS coordinate time series. This study proposes a wavelet-based hybrid method to eliminate the flicker noise as well as the white noise contained in GPS coordinate time series based on wavelet theory. The main conclusions can be summarized as follows:

1. The noise in GPS coordinate time series involves not only the white noise but also the flicker noise. Furthermore, the presence of the flicker noise can easily lead to a seriously destructive interference to understand the real historical deformation processes or to predict the probable future displacement trends as the white noise does.
2. The utility of the wavelet-based hybrid approach to eliminate flicker and white noise in GPS coordinate time series proved to be more comprehensive than that of the classical methods (e.g., wavelet thresholding, wavelet shrinkage denoising, and Kalman filters). Thorough analysis exhibits the superiority of the proposed algorithm with respect to the smoothness as well as to the SNR of the signal.
3. The advance elimination of the flicker noise is beneficial to the wavelet thresholding process when

we make use of it to remove the white noise in GPS coordinate time series.

Despite the achievements in this research, there are still some aspects that need to be further investigated, especially when more coordinate time series from other global navigation satellite systems (e.g., GLONASS of Russia, Galileo of Europe, Beidou of China, and other regional systems) are available. We cannot completely exclude the possibility that other errors, such as random walk noise, exist among the above-mentioned satellite navigation datasets or their combinations (Shi et al. 2013; Niu et al. 2014). After all, the noise situation with respect to GNSS-based coordinate time series becomes more complicated than that of the sole-GPS navigation under the circumstance that the multi-constellation receiver is now in operation in many fields. Given the precise requirements in applying coordinate time series derived from these multi-constellation receivers, it is essential for us to develop more novel methods to analyze other kinds of noises to improve the application reliability of coordinate time series from various global navigation satellite systems.

Acknowledgments This work is supported by the National Natural Science Foundation of China (40901214 and 41301588), the China Postdoctoral Science Foundation (2013M 531749, 2012T50691), the Hong Kong Scholars Program (XJ2012036), the Hong Kong Polytechnic University under Projects (G-YZ26), the Fundamental Research Funds for the Central Universities (2013-IV-040), and the self-determined and innovative research funds of WUT (20131049708009). Additionally, we are grateful to American Journal Experts for English editing of the manuscript. The helpful comments and suggestions from two anonymous reviewers are very gratefully acknowledged.

References

Agnew DC (1992) The time-domain behavior of power-law noises. Geophys Res Lett 19(4):333–336

Amiri-Simkooei AR (2009) Noise in multivariate GPS position time-series. J Geodesy 83(2):175–187

Amiri-Simkooei AR, Tiberius CCJM (2007) Assessing receiver noise using GPS short baseline time series. GPS Solut 11(1):21–35

Amiri-Simkooei AR, Tiberius CCJM, Teunissen PJG (2007) Assessment of noise in GPS coordinate time series: methodology and results. J Geophys Res 112:B07413. doi:10.1029/2006JB004913

Azzalini A, Farge M, Schneider K (2005) Nonlinear wavelet thresholding: a recursive method to determine the optimal denoising threshold. Appl Comput Harmon Anal 18(2):177–185

Chen BS, Lin CW (1994) Multiscale Wiener filter for the restoration of fractal signals: wavelet filter bank approach. IEEE Trans Signal Process 42(11):2972–2982

Donoho DL (1995) De-noising by soft-thresholding. IEEE Trans Inf Theory 41(3):613–627

Donoho DL, Johnstone JM (1994) Ideal spatial adaptation by wavelet shrinkage. Biometrika 81(3):425–455

Fu Z (2001) Information theory-fundamental theory and application. Publishing House Of Electronics Industry, Beijing

Gao HY (1997) Choice of thresholds for wavelet shrinkage estimate of the spectrum. J Time Ser Anal 18(3):231–251

Geng Y, Wang J (2008) Adaptive estimation of multiple fading factors in Kalman filter for navigation applications. GPS Solut 12(4):273–279

Han M, Liu Y, Xi J, Guo W (2007) Noise smoothing for nonlinear time series using wavelet soft threshold. IEEE Signal Process Lett 14(1):62–65

He K, Wang SX (2003) Study on denoising of fractal signal based on Shannon entropy. In: Proceedings of 2003 International Conference on Neural Networks and Signal Processing, vols 1 and 2. IEEE, New York, pp 751–755

Huang L, Fu Y (2007) Analysis on the noises from continuously monitoring GPS sites. Acta Seismol Sin 29(2):197–202

Langbein J, Johnson H (1997) Correlated errors in geodetic time series: implications for time-dependent deformation. J Geophys Res 102(B1):591–603

Leick A (2004) GPS satellite surveying. Wiley, Hoboken

Ma L, Shi Y, Yu H (2002) Studying on denoising of chaotic signal using wavelet transform. Signal Process 18(1):83–87

Mandelbrot BB (1983) The fractal geometry of nature. W.H. Freeman, New York

Mao A, Harrison CG, Dixon TH (1999) Noise in GPS coordinate time series. J Geophys Res 104(B2):2797–2816

Montillet JP, Tregoning P, McClusky S, Yu K (2013) Extracting white noise statistics in GPS coordinate time series. IEEE Geosci Remote Sens Lett 10(3):563–567

Nikolaidis R, Bock Y, de Jonge PJ, Shearer P, Agnew DC, Domselaar M (2001) Seismic wave observations with the global positioning system. J Geophys Res 106(B10):21897–21916

Niu X, Chen Q, Zhang Q, Zhang H, Niu J, Chen K, Shi C, Liu J (2014) Using Allan variance to analyze the error characteristics of GNSS positioning. GPS Solut 18(2):231–242

Santamaria-Gomez A, Bouin M-N, Collilieux X, Woeppelmann G (2011) Correlated errors in GPS position time series: implications for velocity estimates. J Geophys Res 116:B01405. doi:10.1029/2010jb007701

Senior KL, Ray JR, Beard RL (2008) Characterization of periodic variations in the GPS satellite clocks. GPS Solut 12(3):211–225

Shannon CE (1948) A mathematical theory of communication. Bell Syst Tech J 27:379–423

Shi C, Gu S, Lou Y, Ge M (2012) An improved approach to model ionospheric delays for single-frequency precise point positioning. Adv Space Res 49(12):1698–1708

Shi C, Yi W, Song W, Lou Y, Zhang R (2013) GLONASS pseudorange inter-channel biases and their effects on combined GPS/GLONASS precise point positioning. GPS Solut 17(4):439–451

Souza E, Monico J (2004) Wavelet shrinkage: high frequency multipath reduction from GPS relative positioning. GPS Solut 8(3):152–159

Teferle FN, Williams SDP, Kierulf HP, Bingley RM, Plag HP (2008) Acontinuous GPS coordinate time series analysis strategy for highaccuracy vertical land movements. Phys Chem Earth 33(3):205–216

Tregoning P, Watson C (2011) Correction to "Atmospheric effects and spurious signals in GPS analyses". J Geophys Res 116(B2):B02412. doi:10.1029/2010JB008157

Wang Z, Zhang H, Sun J (2011) Framework and case study on geospatial knowledge discovery based on spatial knowledge management. In: Eighth international conference, fuzzy systems and knowledge discovery (FSKD). IEEE, Shanghai, pp 1280–1284. doi:10.1109/FSKD.2011.6019709

Williams SDP (2008) CATS: GPS coordinate time series analysis software. GPS solut 12(2):147–153

Williams SDP, Bock Y, Fang P, Jamason P, Nikolaidis PM, Prawirodirdjo M, Miller M, Johnson DJ (2004) Error analysis of continuous GPS position time series. J Geophys Res 109(B3):B03412. doi:10.1029/2003JB002741

Wornell GW, Oppenheim AV (1992) Estimation of fractal signals from noisy measurements using wavelets signal processing. IEEE Trans Signal Process 40(3):611–623

Wu H, Li Y, Chen N, Xiao S, Cui W (2011) A grid-based remote monitoring and diagnosis system for the railway roadbed roller compaction. Adv Sci Lett 4(8–10):3233–3237

Wu H, Tao J, Li X, Chi X, Li H, Yang R, Wang S, Chen N (2013) A location based service approach for collision warning systems in concrete dam construction. Saf Sci 51(1):338–346

Zhang Q, Aliaga-Rossel R, Choi P (2006) Denoising of gamma-ray signals by interval-dependent thresholds of wavelet analysis. Meas Sci Technol 17(4):731–735

Zhao G, Pei H, Liang H (2013) Measurement of additional strains in shaft lining using differential resistance sensing technology. Int J Distrib Sens Netw. doi:10.1155/2013/153834

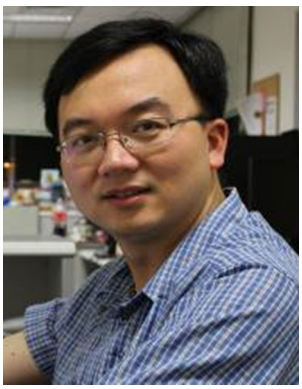

Hao Wu is an Associate Professor at the School of Resources and Environmental Engineering, Wuhan University of Technology. He received the PhD degree from State Key Laboratory of Information Engineering in Surveying, Mapping and Remote Sensing, Wuhan University, in 2007. His research interests focus on Geomatics, hazard monitoring and prediction with GNSS, and Earth observation science.

Kui Li is a postgraduate student of Wuhan University of Technology. He received his bachelor's degree in Changzhou University in 2013. His current research interests include hazard monitoring with GNSS and safety science in mining engineering.

Wenzhong Shi is a Chair Professor and Head of Department of Land Surveying and Geo-Informatics, The Hong Kong Polytechnic University. He received the PhD degree from University of Osnabruck in Vechta, Germany, in 1994. His current research interests include uncertainty and spatial data quality control, hazard monitoring with GNSS and prediction through geodetic means, and GIS and remote sensing.

Keith C. Clarke is a Professor at Department of Geography, University of California, Santa Barbara. He received the PhD degree from The University of Michigan in 1983. His current research interests include environmental simulation modeling, modeling urban growth using cellular automata, and Earth observation science.

Jianhua Zhang is a Professor and Head of Department of Mining Engineering, Wuhan University of Technology. He received the PhD degree from Beijing Institute of Technology in 2000. His current research interests include mining engineering, hazard monitoring with GNSS and prediction through geodetic means, and Geomatics.

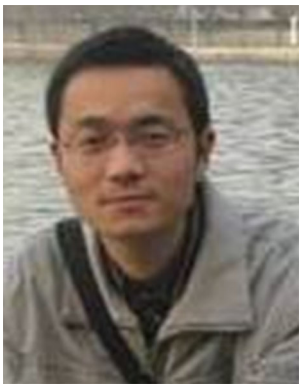

Hua Li is an Associate Professor at the School of Resources and Environmental Engineering, Wuhan University of Technology. He received the PhD degree from The Guangzhou Institute of Geochemistry of the Chinese Academy of Sciences (GIGCAS) in 2006. His research interests include the integration of GNSS and GIS, hazard monitoring, and prediction.